# The Arequipa massif of Peru: new SHRIMP and isotope constraints on a Paleoproterozoic inlier in the Grenvillian orogen.

**C. Casquet[a,*], C.M. Fanning[b], C. Galindo[a], R.J. Pankhurst[c], C. Rapela[d], P.Torres[e]**

[a] *Dpto. Petrología y Geoquímica, Fac.Ciencias Geológicas, Inst. Geología Económica. (CSIC, Universidad Complutense), 28040 Madrid, Spain*

[b] *Research School of Earth Sciences, The Australian National University, Canberra, ACT 200, Australia.*

[c] *British Geological Survey, Keyworth, Nottingham NG12 5GG, UK*

[d] *Centro de Investigaciones Geológicas, Universidad de La Plata, 1900, La Plata, Argentina.*

[e] *Universidad Nacional de Ingeniería, Av. Tupac Amaru 210, Lima, Perú*

- *Corresponding author. Tel. +34 913944908; fax: +34 91
- E-mail address: casquet@geo.ucm.es

## Abstract

The enigmatic Arequipa massif of southwestern Peru is an outcrop of Andean basement that underwent Grenvillian-age metamorphism. It is thus important to better constrain Laurentia–Amazonia ties in Rodinia reconstruction models. U-Pb SHRIMP zircon dating has yielded new evidence on the evolution of the massif between Middle Paleoproterozoic and Early Paleozoic. The oldest rock-forming events occurred in major orogenic events between *ca*. 1.79 and 2.1 Ga (Orosirian to Rhyacian), involving early magmatism (1.89–2.1Ga),

presumably through partly Archaean continental crust, sedimentation of a thick sequence of terrigenous sediments, UHT metamorphism at *ca*. 1.87 Ga, and late felsic magmatism at *ca*. 1.79 Ga. The Atico sedimentary basin developed in the Late Mesoproterozoic and detrital zircons were fed from a source area similar to the high-grade Paleoproterozoic basement but also from an unknown source that provided Mesoproterozoic zircons of 1200–1600 Ma. The Grenville-age metamorphism was of low P-type and reworked the Paleoproterozoic rocks and also affected the Atico sedimentary rocks. Metamorphism was diachronous: *ca*. 1040 Ma in the Quilca and Camaná areas and in the San Juán Marcona domain, 940 ± 6 Ma in the Mollendo area, and between 1000 and 850 Ma in the Atico domain. These metamorphic domains are probably tectonically juxtaposed. Comparison with coeval Grenvillian processes in Laurentia and in southern Amazonia opens the possibility that Grenvillian metamorphism in the Arequipa massif resulted from extension and not from collision. The Arequipa massif experienced Ordovician–Silurian magmatism at ca. 465 Ma, including anorthosites formerly considered to be Grenvillian, and high-T metamorphism within the magmatic arc. Focused retrogression along shear zones or unconformities took place between 430 and 440 Ma.

**Key words:** Arequipa, Grenvillian orogeny, Paleoproterozoic, U-Pb SHRIMP zircon dating, Rodinia.

## Introduction

The Arequipa Massif (Cobbing and Pitcher, 1972) is an outcrop of metamorphic rocks and cross-cutting batholiths at least 800 km long and 100 km wide, along the desert coast of southern Peru (Shackleton et al., 1979), between the Andean Cordillera and the Chile–Peru trench (Fig. 1). It is part of the Andean basement that outcrops both as discontinuous inliers

throughout the belt and in uplifted blocks in the Andean foreland, from as far north as Venezuela to as far south as the Sierras Pampeanas of Argentina (see Rapela et al., this volume). Metamorphic rocks of the Arequipa Massif are mostly metasedimentary and range from amphibolite to granulite facies. Pervasive retrogression under greenschist facies was focused within late strongly sheared zones. Early dating of granulites between Camaná and Mollendo (Fig. 1) by Rb-Sr (whole-rock isochrons) and U-Pb (bulk dating of zircons) first resulted in Precambrian ages of ca 1.8–1.95 Ga (Cobbing et al., 1977; Dalmayrac et al., 1977; Shackleton et al., 1979). Regional metamorphism in the Arequipa Massif according to these authors resulted from a single Paleoproterozoic tectonothermal event; the age of sedimentary protoliths was estimated at *ca*. 2000 Ma. Emplacement of plutons and metamorphic reworking under low-grade conditions took place in the Paleozoic at *ca*. 450 Ma and *ca*. 390 Ma (Shackleton et al., 1979).

Paleogeographic models of Proterozoic continents as developed in the 1990s led to a renewed interest in the study of the Arequipa Massif. According to these models most continental masses reunited into a large supercontinent called Rodinia by the end of the Mesoproterozoic as a result of the Grenvillian orogeny (e.g. Moores, 1991; Hoffman, 1991; Dalziel, 1997). In these models, and in more recent paleogeographical reconstructions, the Amazonia craton figures juxtaposed to Laurentia, i.e., the ancestral North America craton, at *ca*. 1.0 Ga, although their relative positions vary from one to another (e.g., Dalziel, 1997; Davidson, 1995; Loewy et al., 2003; Tohver et al., 2004; Li et al., 2008). Amazonia broke away from Laurentia in the Neoproterozoic, leading to the opening of the Iapetus Ocean and the intervening Grenvillian orogen broke into conjugate belts along the margins of the rifted continents. Because Grenvillian ages were known from elsewhere in South America, lending credence to the Laurentia - Amazonia connection in this way, the age, paleogeography and

tectonics of the Arequipa Massif became the subject of thorough isotope (Nd and Pb) and renewed geochronological research (Wasteneys et al., 1995; Tosdal, 1996; Bock et al., 2000; Loewy et al., 2003, 2004).

U-Pb single-grain zircon dating of granulites yielded Grenvillian ages of *ca*. 1200 Ma near Quilca, and ca 970 Ma near Mollendo for the high-grade metamorphism, with protolith ages of *ca*. 1.9 Ga (Wasteneys et al., 1995). The age of regional metamorphism in the Arequipa Massif thus switched from Paleoproterozoic to Late Mesoproterozoic and the massif was re-interpreted as having originated within the Grenville province. Further conventional zircon U-Pb dating was carried out by Loewy et al. (2004) on igneous gneisses of the San Juán and Mollendo areas. They inferred a complex history of crystallization of protoliths between 1851 and 1818 Ma, and at *ca*. 1790 Ma, with development of an earlier gneissic fabric prior to the latter (M1 metamorphism). Mesoproterozoic metamorphism (M2) took place between *ca*. 1052 Ma at San Juán and 935 Ma near Mollendo, suggesting a north-to-south younging of the metamorphic peak. A retrograde metamorphic overprint (M3) and conspicuous granite magmatism took place in the Ordovician at *ca*. 465 Ma (Loewy et al., 2003). Martignole and Martelat (2003) focused on the structure, geochronology and mineralogy of the high-grade metamorphism between Camaná and Mollendo, which they classified as of the UHT type (T>900 ºC; 1.0–1.3 GPa) on account of ubiquitous peak assemblages with orthopyroxene+sillimanite+quartz and the local coexistence of sapphirine+quartz. Dating this metamorphism was attempted by *in situ* chemical (CHIME) U-Th-Pb determinations on monazites; the calculated ages range from 1064 to 956 (±50) Ma, with a peak *ca*. 1.0 Ga.

The Arequipa Massif has long been considered to be the northern exposure of a larger hypothetical continental block that outcrops as basement inliers within the Andean Cordillera

in northern Chile and northern Argentina, i.e., the composite Arequipa-Antofalla craton (Ramos, 1988). This block includes a Grenvillian basement and post-Grenvillian metamorphic and igneous overprints as young as 0.4 Ga (Loewy et al., 2003). Isotope (Nd and Pb) and geochronological considerations led Casquet et al. (2008) to establish comparisons between Grenvillian terranes recognized in the Western Sierras Pampeanas, i.e., the Andean foreland, and the Arequipa Massif, thus enlarging the boundaries of the Arequipa-Antofalla block. However, both the role of the Arequipa Massif in the Grenvillian orogeny and its pre-Grenvillian history are still poorly known. Wasteneys et al. (1995) were the first to propose that the Arequipa Massif was a promontory of Laurentia accreted to Amazonía during the Sunsás orogeny, a Late Mesoproterozoic Grenvillian-age tectonic event long recognized along the SW margin of Amazonía, in Brasil and SE Bolivia (Litherland et al., 1989; Cordani and Teixeira, 2007). According to Wasteneys et al. (1995) granulite metamorphism resulted from pre-collisional subcontinental mantle delamination coeval with flat subduction, and concomitant rise of the hot asthenosphere that heated the overlying continental crust (see also Martignole and Martelat, 2003). However, for Loewy et al. (2004) the Arequipa-Antofalla block was an orphaned block, accreted to Amazonia during the Sunsás orogeny at *ca*. 1.05 Ga.

It is now widely accepted that the Grenvillian orogenic cycle played an important role in Central Andean South America as evidenced by the Arequipa Massif and the Western Sierras Pampeanas. Moreover Grenvillian-age rocks have long been recognized in the basement of the Northern Andes (e.g., Restrepo Pace et al., 1997) and along the southern margin of the Amazonia craton (Cordani and Teixeira, 2007). However the pre-Grenvillian history and the time and mode of accretion of the Grenvillian terranes to nearby Amazonia, and correlations with the alleged Laurentian conjugate margin, still remain speculative.

This contribution is aimed at better constraining the igneous and metamorphic history of the Arequipa Massif by means of new U-Pb SHRIMP determinations and complementary geochemical evidence. We conclude that the massif was the site of a complex history that consisted of sedimentation, magmatism and metamorphism (UHT) in the Paleoproterozoic, development of a sedimentary basin in the Mesoproterozoic, Grenville-age medium- to high-grade metamorphism, and local metamorphic reworking and magmatism in the Early Paleozoic.

## Geological setting

The most comprehensive geological description of the Arequipa Massif is that of Shackleton et al. (1979). We retain here some of the domains that they distinguished to better locate our samples. A summarized description follows based on their work and our own observations.

### The northern section

The *San Juán Marcona area* in the north (Fig. 1) consists of a basement and a discordant cover sequence. The latter is formed by glacial diamictites of the Chiquerio Formation followed by a carbonate cap, the San Juán Formation, both probably Neoproterozoic (Chew et al., 2007). The basement consists of banded migmatitic gneisses and minor fine-grained gneisses, strongly dismembered concordant pegmatites, concordant and discordant amphibolite dykes, and a foliated megacrystic granite of *ca*. 1790 Ma (Loewy et al., 2003). Late granitic plutons cutting the discordance are Ordovician (Loewy et al., 2003). The *Atico*

*domain*, between Atico and Ocoña is medium-grade, with staurolite (+andalusite; Shackleton et al., 1979) schists, grey metasandstones, variably retrogressed amphibolites and concordant pegmatite sheets. Southward, this domain merges into a low-grade zone, *the Ocoña phyllonite zone*, that consists of strongly strained greenish chlorite-muscovite schists, grey metasandstones, quartz veins and concordant foliated pegmatite bodies. Shear bands, i.e., S-C′ structures, are widespread and suggest that this is a shear zone with a top-to-the-NE sense of movement. Relics of an older foliation with discordant pegmatite dykes are locally preserved in strain shadows, outside which pegmatites are transposed to parallelism with the shear foliation. This shear zone was attributed to Paleozoic tectonism, probably Devonian, on structural grounds only (Shackleton et al., 1979). However, one foliated granite within the zone yielded an Ordovician age of *ca*. 464 Ma that is argued by Loewy et al. (2003) as shortly prior to the low-grade metamorphism (M3). The large *Atico igneous complex* consists in large part of diorites variably retrogressed to chlorite - epidote - albite, and abundant pegmatite dykes. This complex, along with its southern prolongation in the Camaná Igneous Complex, was attributed an age of *ca*. 450 Ma by Shackleton et al. (1979) on the basis of a combined Rb-Sr whole-rock isochron.

The southern section

The *Camaná–Mollendo domain* is the largest one and consists of high-grade rocks that underwent granulite facies UHT metamorphism, with a paragenesis containing orthopyroxene+sillimanite+quartz and sapphirine+quartz (Martignole and Martelat, 2003). It consists for the most part of monotonous banded migmatitic gneisses formed by variably restitic mesosomes and alternating leucosomes (Fig. 2a). Augen-gneisses are found locally, such as near Mollendo, that probably formed by stretching of banded migmatites within

strongly strained shear zones. Peneconcordant but unstrained muscovite pegmatite sheets are irregularly distributed throughout the domain, more abundant in the north and northwest between Quilca and Camaná. Foliation is very regular over long distances. However changes in dip and strike can be mapped on a regional scale due to large upright post-foliation folds. Small-scale (cm to m) syn-foliation folds are locally found.

The Ilo domain

The southernmost *Ilo domain* is separated from the main massif by a cover of Mesozoic and Cenozoic sedimentary rocks. This domain is a medium- to low-grade shear zone with strongly retrogressed igneous protoliths. The main facies is reddish, variably foliated, porphyritic granite. Boudins of coarse anorthosite that resulted from stretching of older larger bodies are aligned within the foliated porphyritic granite. A third facies consists of narrow bands, parallel to foliation, of a dark fine-grained mylonitic rock that contains irregularly distributed feldspar porphyroclasts. Contacts are sharp or gradual. Some bands look like sheared porphyritic granites; others as appear to be derived from dykes that underwent local mingling with the host granite. Strain increases from anorthosite through the dark bands to the granite; mylonitic foliation is common (Fig. 2b). Martignole et al. (2005) considered the protoliths to be part of a Grenvillian AMCG suite.

**Sampling and petrographic description**

Out of a larger sampling of the whole massif from San Juán down to Ilo, eight samples were chosen for U-Pb SHRIMP dating of zircons and eight for Nd isotope composition. Two

muscovite samples were collected from pegmatites. Sampling was aimed at deciphering the complex geological history of this basement and particularly to constrain the age of the Grenvillian tectonothermal event. Because of the tectonic implications and the expected influence of the alleged Grenvillian anorthosite magmatism in UHT metamorphism (e.g., Arima and Gower, 1991, and references therein) one target was the anorthosite and allied rocks from Ilo. Determining the protoliths of many of the metamorphic rocks was difficult, particularly for the highly recrystallized rocks of the Camaná–Mollendo domain, and so five high-grade gneisses from this domain were also analysed for REE.

Sample locations are shown in Fig. 1. Coordinates, description, abbreviated mineralogy and the analytical work carried out on each sample are shown in Table 1. More detailed petrographic descriptions of the rocks can be found in Supplementary Table 1, obtainable from the Journal of South American Earth Sciences supplementary data file #1.

**Analytical methods**

REEs were analysed at ACTLABS (Canada) by ICP-MS (Table 4). Samples for Sr and Nd isotope analysis were crushed and powdered to ~ 200 mesh. Powders were first decomposed in 4 ml HF and 2 ml $HNO_3$ in Teflon digestion bombs for 48 hours at 120 ºC, and finally in 6M HCl. Elemental Rb, Sr, Sm and Nd were determined by isotope dilution using spikes enriched in $^{87}Rb$, $^{84}Sr$, $^{149}Sm$ and $^{150}Nd$. Ion exchange techniques were used to separate the elements for isotopic analysis. Rb, Sr and REE were separated using Bio-Rad AG50 x 12 cation exchange resin. Sm and Nd were further separated from the REE group using Bio-beads coated with 10% HDEHP. All isotopic analyses were carried out on a VG Sector 54

multicollector mass spectrometer at the Geocronología y Geoquímica Isotópica Laboratory, Complutense University, Madrid, Spain. Nd and Sr isotope data are shown in Tables 2 and 3 respectively.

U-Pb analyses were performed on eight samples using SHRIMP RG at the Research School of Earth Sciences, The Australian National University, Canberra. Zircon fragments were mounted in epoxy together with chips of the Temora reference zircon, ground approximately half-way through and polished. Reflected and transmitted light photomicrographs, and cathodo-luminescence (CL) SEM images, were used to decipher the internal structures of the sectioned grains and to target specific areas within the zircons. Each analysis consisted of 6 scans through the mass range. The data were reduced in a manner similar to that described by Williams (1998, and references therein), using the SQUID Excel macro of Ludwig (2001). U-Pb data are in Supplementary Table 2 obtainable from the Journal of South American Earth Sciences Data Files 2#. Results are shown in Figs 3-5 and described below.

**Zircon SHRIMP U-Pb samples and results**

*MAR-8***.** Fine-grained gneiss (meta-igneous) (Fig. 3a). Zircons are elongate (less than 150μm in length) sub-rounded to euhedral in shape. CL images show that most grains consist of a core and a rim. Cores are elongate euhedral prisms, although with resorption features, with oscillatory zoning that reflects an igneous origin. Rims show low luminescence and are large enough to be analysed.

Eighteen points were analysed including rims and cores. Nine cores yielded $^{207}Pb/^{206}Pb$ ages between 1210 and 1813 Ma. If analyses with discordance > 10% are rejected (#12 & #17), the remaining spots plot near Concordia and yield a mean $^{207}Pb/^{206}Pb$ age of 1796±13 Ma (MSWD = 1.5), which is interpreted as the crystallization age of the igneous protolith. The high Th/U values of cores (0.32–0.34), typical of igneous zircons, reinforce this interpretation. Rims are high-U (mostly over 1000 ppm) and with very low Th/U values (mostly <0.2) typical of a metamorphic origin. Rim analyses plot on a discordia with an upper intercept at 1033±23 Ma and a lower intercept at 469±70Ma; taken as the ages of Grenvillian metamorphism and early Paleozoic overprint, respectively. The latter gave rise to more pronounced Pb-loss in the Grenvillian rims than in the relict cores.

*OCO-26*. Meta-sandstone (Fig. 3b). The zircons from this sample are mostly equant, round to sub-round grains that range up to 200 μm in diameter but with many less than 50–100μm. The grains are generally clear and colourless, with only some clouded grains, and some that may be frosted due to surface transport. The CL images reveal a complex internal structure (Fig. 3b). Many grains comprise a zoned igneous centre, overgrown by metamorphic zircon with homogeneous CL. Also common are grains with metamorphic central areas with lighter or darker CL outermost metamorphic zircon. Some grains have multiple stages of zircon growth, the outermost invariably being a bright CL metamorphic rim.

Given the complex nature of the zircon population, 105 areas were analysed on 70 zircon grains. The analyses range up to 30% discordant, although many are within analytical uncertainty of both the Wetherill ($^{204}Pb$-corrected data) and Tera-Wasserburg concordias (data uncorrected for common Pb). The relative probability plot shows a major peak at 1000 Ma, with slightly younger subordinate groups of analyses at *ca*. 940 Ma and *ca*. 840 Ma, a

sequence of minor peaks through the Mesoproterozoic (*ca*. 1200, 1260, 1340, 1500), and a significant concentration in the interval 1650–2030 Ma, as well as a few older ages back to 2770 Ma (Archaean). The older ages are comparable to those seen in other samples reported here. We interpret the major peak at *ca*. 1000 Ma as corresponding to peak metamorphism of Grenville-age in the Atico domain. All older ages are interpreted as reflecting detrital grains, mostly igneous, but also metamorphic mantles.

The data giving the youngest ages tend to plot above the Concordia curve in the Tera-Wasserburg diagram (not shown), in part forming a Pb-loss discordia. These areas are considered to have lost radiogenic Pb and are not interpreted as reflecting Neoproterozoic metamorphic zircon. However, the presence of ages of 850–950 Ma in the analyses of the outer areas and rims to structured grains record mean that a case can be made for metamorphic zircon development later than 1000 Ma.

On the basis of this interpretation, peak metamorphism occurred at *ca*. 1000 Ma and the sedimentary protolith may well have formed between this time and the next oldest minor peak at *ca*. 1200 Ma, i.e., Late Mesoproterozoic.

*CAM 2*. Migmatitic gneiss (mesosome) (Fig 4a). The zircons from this sample are equant to elongate, round to subround in shape and less than 200 μm in length. The CL images reveal a range of internal structures. Some areas are zoned igneous zircon, whilst other areas have an irregular wispy structure, and yet others areas are broad and homogeneous. These features indicate a range of zircon crystallization events from simple igneous crystallization, to recrystallized zones and then finally metamorphic zircon growth.

Twenty-four areas were analysed on 21 zircon grains covering the range of internal CL structures, and yielding a bimodal distribution. In general the zoned igneous zircon yields older Proterozoic dates, whereas the more homogeneous metamorphic areas yield Grenvillian dates. But this is not always the case: the outer more homogeneous areas on grains #16 and #18 both yield older Proterozoic dates, whilst the weakly zoned area analysed on grain #17 is Grenvillian in age. Centres and rims were analysed on grains #10, #15 and #21. Both areas on grain #10 yield concordant Grenville dates, though the irregularly zoned core (#10.2) is older than the homogeneous metamorphic rim (#10.1). The irregularly zoned core of grain #15 is *ca*. 1960 Ma whereas the homogeneous rim is *ca*. 1050 Ma. The zoned core of grain #21 is *ca*. 1890 Ma, with the homogeneous rim Grenvillian at *ca*. 1040 Ma.

Overall, the older group consists of igneous and perhaps metamorphic core zircon with a range of nearly concordant $^{207}Pb/^{206}Pb$ ages of 1760 –1950 Ma, but with a composite peak at *ca*. 1900 Ma. The Grenvillian metamorphic group is rather variable with, at the older end, one concordant age at 1125 Ma and one less so at *ca*. 1210 Ma, and at the younger end, two $^{206}Pb/^{238}U$ ages less than 1000 ma that probably indicate either Pb-loss of Grenvillian areas or a superimposed thermal event peaking at *ca*. 980 Ma. The weighted average of the six remaining $^{206}Pb/^{238}Pb$ ages is 1040±11 (MSWD = 0.90), which is taken as the peak of Grenvillian metamorphism.

*CAM-7*. Migmatitic gneiss (mesosome) (Fig 4b). The zircons from this sample are round, equant-to-elongate grains that range from less than 100 μm in diameter to 200μm or more in length. A few multi-lobate grains are present, representing metamorphic overgrowths. The CL images, as of sample CAM 2 show a variety of textures and features. There are areas of

zoned igneous zircon, usually more centrally located within the grains, with both irregular and homogenous CL structures in outer areas (mantles) and rims.

Twenty-seven areas have been analysed on 20 zircon grains with rim-and-core pairs analysed for seven grains. The zoned igneous core to grain #17 has an Archaean $^{207}Pb/^{206}Pb$ age of ~2690 Ma whereas the more homogeneous rim area, interpreted as metamorphic, is Grenvillian in age with a $^{206}Pb/^{238}U$ date of ~1120 Ma. The outer areas and zoned igneous zircons provide a range of nearly concordant $^{207}Pb/^{206}Pb$ dates, mostly around 1860 to 2080 Ma. The Wetherill plot for the $^{204}Pb$-corrected data clearly shows that whilst some areas are near Concordia at about either 1950 Ma or 1000 Ma, many of the areas analysed are discordant and would lie on a simple discordia between these two end-members. A discordia line fitted to a selected group of 22 analyses gives an upper intercept of 1924±25 Ma and lower intercept of 1026±32 Ma (MSWD = 3.7), the latter being taken as the age of peak Grenvillian metamorphism. The analyses not included in this general discordia line are for #15.2, with the youngest $^{207}Pb/^{206}Pb$ date, and those with $^{207}Pb/^{206}Pb$ dates older than 2000 Ma.

From the current data set it is clear that detrital igneous zircon and probably overgrowths of Paleoproterozoic age are common in this sample. New zircon formed during a Grenville-age event is present. A number of the grains/areas analysed show variable radiogenic Pb-loss at this time and so lie on a discordia trend.

*QUI-16*. Migmatitic gneiss (mesosome) (Fig. 4c). Separated zircons are mostly *ca*. 200 μm in length, equant to slightly elongated, and sub-round in form. CL images show complex internal structures, with small relict cores (in some cases with igneous zoning) surrounded by

mantles of variable thickness most of which show broad faint oscillatory zoning, and low-luminiscence rims. The latter are usually complete and discordant to the earlier structures; they are of irregular thickness, up to 50 μm or more on some grain tips. The textures are interpreted as due to detrital igneous crystals and successive stages, probably two, of metamorphic overgrowth.

Sixteen areas were analyzed on 15 grains. Both core and mantle were analysed in grain #1. Two analyses (# 4 and #8) were carried out on well-developed rims; their $^{207}Pb/^{206}Pb$ ages are 1079 Ma and 1995 Ma. The other spots were on mantles: Th/U ratios are generally high (0.07–3.33, with 12 out of 16 ratios being > 0.2). If the more imprecise analyses are excluded, the rest plot on a simple Discordia (MSWD = 0.9) with an upper intercept at 1861±32 Ma and a poorly defined lower intercept at 1011±73Ma.

*MOL-17*. Augen-gneiss (uncertain protolith) (Fig. 4d). The zircons from this sample are round to subround grains that are generally clear. The CL images show complex internal structure; many grains have zoned igneous cores, interpreted as igneous, overgrown by more homogeneous, probably metamorphic zircon.

Sixteen grains were analysed, with most of the analyses on the more homogeneous outer areas of the grains interpreted as metamorphic. The exceptions are the analyses of grain #16, where the zoned core was also analysed (both core and rim giving Archaean ages of *ca*. 2900 Ma). The analyses are generally low in U and the Th/U ratios range to very high values (0.16–4.06), apart from those of grains #10 and #11 (0.08). The analyses mostly plot on a simple discordia between 1892±62 Ma and 973±82 Ma (MSWD rather high at 2.4). There are a number of discordant analyses, but these do not indicate the presence of intermediate

Mesoproterozoic zircon. The three youngest Grenvillian areas are highly concordant and yield a defined Concordia age of 940±6 Ma (MSWD = 0.004), which is taken as the best age for the Pb-loss and possible metamorphic event. There is a possibility that this rock underwent an older thermal event responsible for the Paleoproterozoic ages of some overgrowths. The ultimate age of the protolith is unknown as insufficient data were obtained from cores.

*ILO-19*. Mylonitic porphyritic granite (Fig. 5a). The abundant zircons in this sample are elongate, mostly ~200 μm in length, or longer, with either subround or pyramidal terminations. Many grains can be seen to be strongly zoned under transmitted light and although many are clear and colourless a few are dark and metamict. CL shows a variety of internal structures. Many grains and areas within grains are simple oscillatory zoned zircon, but there are prominent grains with very irregular internal features and in places these wispy features overprint and cross-cut what is interpreted to be the primary simple igneous zoning.

Twenty-three areas were analysed on 20 grains covering the full range of complex internal CL structures. All 23 analyses yield $^{206}Pb/^{238}U$ ages in the range 415–465 Ma and the relative probability plot shows a broad peak or peaks centred at about 450 Ma. Apart from 3 analyses (#3, #4.1 & #15) the data are low in common Pb and the $^{204}Pb$-corrected data are within uncertainty of concordia. There is no evidence for any Grenville-age event in these zircon grains. There is a wide range in U and Th contents, but the Th/U ratios are moderate to high, reflecting the dominantly igneous nature of the zoned zircon. If the three analyses with high common Pb and all others with >10% discordance are excluded, three possible age peaks can be recognized: *ca*. 460 Ma, *ca*. 446 Ma and ca 432. The younger peak could be related to retrogression within the shear zone (overprinting features in zircon grains) which is strong in

this rock.

*ILO-20*. Dark mylonitic gneiss (Fig. 5b). The zircons from this sample are mostly slender, elongate grains with subhedral terminations. More equant and bulkier elongate grains are also present, tending to be coarser-grained, up to 250μm in length and 50μm in width. The CL images show a complex internal structure. Whilst many grains have length-parallel zoning (interpreted as igneous), more homogeneous, possibly metamorphic, zircon is present both as rims and in places forming anastomosing embayments into the zoned igneous zircon.

Twenty-six areas were analysed on 21 grains ( Fig. 5b). A wide range of the internal structures noted above were analysed, with both the zoned igneous and the more homogeneous areas interpreted as metamorphic analysed on a number of single grains. The resulting data form a dispersed grouping that is dominantly within uncertainty of the Tera-Wasserburg Concordia. Two analyses, #2.2 and #6.1, are more enriched in common Pb; the former yields a young $^{206}Pb/^{238}U$ date of *ca*. 438 Ma and the area analysed is considered to have lost radiogenic Pb. The relative probability plot of $^{206}Pb/^{238}U$ ages shows a dominant bell-shaped peak, which yields a weighted mean age of 464±4 (MSWD = 1.07). It is noteworthy that this grouping includes both zoned igneous and the more homogeneous zircon areas; thus the igneous emplacement and subsequent metamorphic developments in these grains occurred within the analytical uncertainty of 464 Ma. On the older age side, there is a subordinate grouping around *ca*. 480 Ma (four analyses give a mean of 483±7 Ma) and scattered older dates to *ca*. 512 Ma. The central areas to a number of grains were analysed as it was originally presumed that this rock would yield a Grenvillian age. However, whilst there are scattered analyses older than the dominant Ordovician peak, there is no evidence for such a Grenville event.

*ILO-23*. Anorthosite (Fig. 5c). Only a few zircon grains were separated from this sample (7 on the probe mount). They are elongate and range from clear subhedral forms to dark, metamict subhedral grains. The CL images are very dark, but relict igneous zoning can be seen.

Seven areas were analysed on 6 grains; they have high U ranging from 1700 to 3065 ppm, with relatively moderate Th and Th/U ratios in the range 0.08 –0.21. This is on the slightly low side for normal igneous zircon but may reflect late-stage magmatic crystallisation or partial melting. The areas analysed are low in common Pb, but not ideal in terms of zircon clarity or good CL structure. The relative probability plot for the limited number of analyses is irregular, with one clearly older analysis and some skew to the young age side. A weighted mean of the $^{206}Pb/^{238}U$ ages for 5 of the 7 analyses provides an estimated crystallisation date of 464±5 Ma (MSWD = 1.0).

**Pegmatites**

Because Rb is strongly fractionated in muscovite relative to Sr, the $^{87}Sr/^{86}Sr$ ratio in the mineral increases very quickly time and the calculated age is insensitive to the assumed initial values for calc-alkaline magmas. The ages of two muscovite samples obtained in this way were 1000 and 1100 Ma (Table 3), i.e., Grenvillian. These pegmatites, although roughly concordant to their host rocks, do not show evidence for ductile deformation and/or superimposed metamorphism, and the Rb-Sr ages are taken as dating magmatic crystallization.

**REE and Nd isotope data**

REE data for five samples of high-grade gneisses from the Camaná–Mollendo domain (Table 4) are plotted in Fig. 6. They show enrichment in LREE relative to HREE, with $(La/Yb)_N$ values between 13.5 and 24, and a small negative Eu anomaly (Eu/Eu* = *ca*. 0.8). REEs patterns are remarkably similar in the five gneisses suggesting that they were all derived from the same type of protolith. They are also strikingly similar to those of shales, e.g., the North American Shale Composite (Taylor and McLennan, 1988), so that it may be inferred that the gneisses were derived from detrital sedimentary rocks. The small differences among the five rocks analysed here may be attributed to variable melt extraction during migmatization.

Nd isotope composition is available for the five high-grade gneisses (Table 2). They yielded εNdt values of -5.5 to -8.2 at the reference age of 1700 Ma. Nd single-stage depleted-mantle model ages ($T_{DM}$, DePaolo et al. 1981) range between *ca*. 2.3 and 2.5 Ga.

Nd isotope composition is also available for three meta-igneous rocks from the Ilo domain. εNdt values at the reference age of 475 Ma (Table 2) differ significantly from one rock to another: -6.4 (ILO-19), -7.8 (ILO-20) and -3.6 (ILO-23), the latter being for the anorthosite. The value for ILO-20, the mafic gneiss, is less primitive than that of the granite, perhaps indicating different protoliths and not only strain differences between the two rocks as might be argued from field evidence alone.

## Discussion

Two views emerge from these data. 1) The geological history of the Arequipa massif covers a very long period of time, between Paleoproterozoic and Early Paleozoic (Ordovician–Silurian). 2) Three main rock-forming events took place, at widely separated times: in the Paleoproterozoic, in the Late Mesoproterozoic and in the Paleozoic.

### The Paleoproterozoic. An old orogenic history

The protolith of the strongly retrogressed quartzose gneiss MAR-8 from the San Juán Marcona domain was a felsic igneous rock, probably volcanic or subvolcanic. Its age of 1796±13 Ma (Late Paleoproterozoic) coincides with a discordia upper intercept age of 1793±6 Ma found by Loewy et al. (2004) for a retrogressed foliated megacrystic granite nearby (sample U/Pb-3). The age of *ca*. 1.79 Ga thus corresponds to an event of felsic magmatism. Moreover, this age constrains the age of the host metasedimentary rocks that were coeval or older.

Migmatitic gneisses of the Camaná–Mollendo domain, although separated from the San Juán domain by the Atico medium-grade rocks and the Ocoña Phyllonite zone, probably correspond to the same geological domain, although they are generally less retrogressed and appear to contain material older than the igneous protolith in the San Juán Marcona domain. Most of the migmatitic gneisses are probably metasedimentary, as inferred from both the similarity of their REE pattern to those of shales and the high peraluminosity evidenced by the mineral compositions (Martignole & Martelat, 2003).

All the samples contain Paleoproterozoic zircons that underwent a metamorphic overprint of Grenvillian age. Low-discordance Paleoproterozoic ages range from 1.76 to 2.1 Ga. A few scattered Archaean zircons were also found (*ca*. 2.7 Ga in CAM-7, *ca*. 2.9 Ga in MOL-17). Moreover, the Paleoproterozoic ages embrace detrital cores with relict igneous zoning and thick subrounded, homogeneous or weakly concentrically-zoned, overgrowths (mantles). The latter features are common in high-grade metamorphic zircons (Vavra et al., 1999; Corfu et al., 2003). Most of the analysed areas were overgrowths, most of them with Th/U values higher than most metamorphic zircons (which tend to have values < 0.1). This fact however has been also recognized in other high-grade metamorphic areas (e.g., Goodge et al., 2001) and, of particular relevance, in UHT metamorphic regions, e.g., in the Napier Complex, Antarctica (Carson et al., 2002). Such high Th/U values in metamorphic mantles are attributed to U-depletion during UHT metamorphism prior to zircon growth (Black et al., 1986; Carson et al., 2002). We propose that the zircon overgrowths in the Arequipa massif migmatitic gneisses probably resulted from UHT metamorphism in the Paleoproterozoic.

Samples CAM-2 and CAM-7 contain detrital igneous cores of 1890 Ma to 2080 Ma that, along with the few Archaean cores referred to above, suggest magmatic events in the source area of the sedimentary protoliths in the Middle Paleoproterozoic (Rhyacian and Orosirian) and in the Archaean. Most of the analysed zircon areas plot on discordias resulting from Pb-loss during Grenvillian metamorphism, and as most correspond to mantles on older cores, the upper intercept ages probably date metamorphism. The strongest cases are for samples QUI-16 and MOL-17, where only overgrowths were considered for regression; the resulting ages are 1861±32 Ma and 1892±62 Ma, respectively. Thus a metamorphic event at *ca*. 1.87 Ga is inferred for the Paleoproterozoic overgrowths. Whether these Paleoproterozoic overgrowths formed *in situ* or were detrital is more difficult to assess. Zircon grains in samples QUI-16

and MOL-17 show overgrowths that are quite regular and complete around detrital igneous cores (Fig. 4). This might be taken as compatible with overgrowth formation *in situ* and consequently with a metamorphic event in the Camaná-Mollendo domain at *ca*.1.87 Ga. This interpretation strengthens that of Loewy et al. (2004), who argued on geological grounds for a metamorphic event (M1) and deformation at *ca*. 1.8 Ga, i.e., prior to the intrusion of the megacrystic granite (U/Pb3). Consequently, the age of the sedimentary protoliths of the migmatitic gneisses can now be bracketed with some confidence between *ca*. 1.87 and the minimum age of detrital igneous zircons, i.e., *ca*. 1.9 Ga. In consequence sedimentary protoliths formed shortly before metamorphism. Quite similarly Cobbing et al. (1977), Dalmayrac et al.(1977) and Shackleton et al. (1979) argued in favour of a granulite facies regional metamorphism between *ca*. 1.8 and 1.95 Ma, with protolith ages of *ca*. 2000 Ma. However these authors considered that the granulitic gneisses resulted from a single metamorphic event and did not recognize the superimposed Grenvillian event (see below).

Nd isotope values ($T_{DM}$ between *ca*. 2.3 and 2.55 Ga) suggest that Nd in the Camaná-Mollendo migmatitic gneisses is largely reworked from an old continental crustal material, Paleoproterozoic and/or Archaean. This is compatible with the presence in some samples of old detrital zircons of *ca*. 2690 Ma (CAM-7) and *ca*. 2900 Ma (MOL-17) that indicate an Archaean source. Moreover, the crustal source of the zircons experienced magmatism at different times between *ca*. 1.9 and 2.1 Ga, probably with addition of a juvenile component to the upper continental crust. This constitutes a significant fingerprint of the source area, i.e., old Nd model ages and a younger zircon population.

As for the Paleoproterozoic, the pattern that emerges from zircon ages and the geological and geochemical evidence is one of an orogeny between *ca*. 1.79 and 2.1 Ga (Orosirian to

Rhyacian) involving: a) early magmatism (between 1.89 and 2.1Ga), presumably through partly Archaean continental crust, b) sedimentation of a thick sequence of terrigenous sediments, c) UHT metamorphism at *ca*. 1.87 Ga, and d) late felsic magmatism at *ca*. 1.79 Ga.

The Atico domain: a Mesoproterozoic sedimentary basin.

The only sample from this medium-grade metamorphic domain (OCO-26) shows similarities to the migmatitic gneisses of the Camaná–Mollendo domain, but also significant differences. Many low-discordance areas yield ages between 1700 and 2030 Ma and a few are Archaean, between 2600 and 2800 Ma (one discordant age *ca*. 3100 Ma). These ages are from detrital igneous cores and metamorphic mantles, and are similar to the Proterozoic to Archaean low-discordance ages found in the Camaná–Mollendo and San Juán domains. On the other hand, OCO-26 contains zircons with nearly concordant ages between *ca*. 1200 and *ca*. 1600 Ma. This group of ages has not been recognized in the high-grade domains; we interpret these zircons as detrital. Grenvillian metamorphism started at *ca*. 1000 Ma.

Deposition of the sedimentary protolith of OCO-26 occurred between *ca*. 1200 and *ca*.1000 Ma, i.e., in the Late Mesoproterozoic. Detrital zircons were fed from a source area similar to the high-grade Camaná–Mollendo and San Juán domains, but also from an unknown source that provided the Mesoproterozoic zircons of 1200–1600 Ma. The Atico domain can thus be interpreted as a sedimentary basin deposited on a Paleoproterozoic high-grade basement consisting of igneous and metamorphic rocks. Cobbing et al. (1977) first considered the Atico metasedimentary rocks to be younger than the Mollendo high-grade

gneisses because of the presence of quartzites, absent in Camaná–Mollendo domain. However this opinion was challenged by Wasteneys et al. (1995).

The Grenville-age metamorphic event

All the zircon populations from the San Juán, Atico and Camaná-Mollendo samples show the imprint of a metamorphic event Late-Mesoproterozoic to Early Neoproterozoic in age. This metamorphism produced Pb-loss on both older zircon igneous cores and on Paleoproterozoic overgrowths, giving rise to linear discordias, and probably new overgrowths in the form of contrasting luminescence rims. Recorded Grenvillian ages can be bracketed between *ca*. 940 and *ca*. 1080 Ma, taking age uncertainties into account. In the Camaná-Mollendo domain Grenvillian ages are apparently older in the Quilca and Camaná samples (CAM-2: 1040±11 Ma; CAM-7: 1026±32 Ma; QUI-16: 1011±73 Ma) than in the Mollendo sample (MOL-17: 940±6 Ma), a fact that was also recognized by Wasteneys et al. (1995; point C: 966±5 Ma) and by Loewy et al. (2004; sample U/Pb-2: 935±14 Ma). Sample MAR-8 from the San Juán Marcona domain yielded an age of 1033±23 Ma for the Grenvillian event, i.e., within error of those of the southern Camaná-Mollendo domain. The weighted average age of metamorphism in northern Camaná–Mollendo and San Juán Marcona is 1037±19 Ma. In the Atico domain we found a spread of Grenvillian ages between *ca*. 1000 and *ca*. 840 Ma. The latter domain underwent only Grenvillian metamorphism, in contrast with the Camaná–Mollendo domain, which besides Grenvillian metamorphism underwent an older Paleoproterozoic event. Martignole and Martelat (2003) carried out chemical dating of monazites from the Camaná–Mollendo domain and found a spread of Grenvillian ages; statistically meaningful ages of *ca*. 1000 Ma were obtained for three samples near Camaná. Moreover, muscovite pegmatites, probably migmatitic melts, were emplaced during the

Grenvillian event (1000 and 1100 Ma) as inferred from the Sr isotope composition of muscovites presented here.

Grenville-age metamorphism at Arequipa took thus place in as many as three separate episodes: 1) *ca*. 1040 Ma in the Quilca and Camaná areas of the Camaná–Mollendo domain, and in the San Juán Marcona domain, 2) at 940±6 Ma in the Mollendo area of the Camaná-Mollendo domain; 3) between *ca*. 1000 and 840 Ma in the Atico domain. This evidence suggests that in the Arequipa massif metamorphic domains are juxtaposed that underwent Grenvillian metamorphism at different times and had different cooling histories.

It is difficult to distinguish the effects of the Grenvillian metamorphic overprint on the older UHT paragenesis. Martignole & Martelat (2003), although favouring a single metamorphism of Grenville-age, leave this question open, suggesting that this might correspond to the lowest-P event (T<900ºC) they recognized. In our hypothesis that the UHT metamorphism in Arequipa was Paleoproterozoic, temperatures attained during Grenvillian metamorphism had to be high enough to completely reset the Th-U-Pb system in monazites (*ca*. 730ºC; Copeland et al., 1988; Parrish, 1990) unless the monazite formed only during the Grenvillian event. Moreover Grenville-age Ms-pegmatites are evidence for renewed partial melting at this time. Temperatures between 730º and 900ºC were thus probably attained during Grenvillian metamorphism in the Camaná–Mollendo domain. In the Atico domain however, Grenvillian metamorphism only attained P-T values within the stability field of staurolite+andalusite (Shackleton et al., 1979) implying a low-pressure type of metamorphism.

Paleozoic events: the Ordovician magmatic arc

Ordovician crystallization ages found here for the igneous protoliths of the Ilo domain were unexpected. Martignole et al. (2005) interpreted these rocks as a Grenvillian AMGC (anorthosite-mangerite-charnockite-granite) suite on the basis of locally preserved relict high-temperature minerals such as pyroxenes and alleged metamorphic garnet, and Nd model ages of *ca*. 1.15 Ga. In our samples those minerals are absent. However minerals such as hornblende, biotite and rutile (in anorthosite) are preserved in the less retrogressed rocks (ILO-20 and ILO-23) and also argue in favour of an earlier high-temperature history including igneous crystallization in a deep magma chamber and metamorphism. The latter, which is evidenced by zircon overgrowths on igneous cores (e.g., ILO-20), took place within the analytical uncertainty of the crystallization ages. Ages of igneous zircons of *ca*. 460 Ma place this magmatism within the Famatinian orogenic cycle, well-known in NW Argentina, which took place along the proto-Andean margin of Gondwana (Pankhurst et al., 2000; Dahlquist et al., 2008, and references therein). Loewy et al. (2004) obtained U-Pb ages between 440 and 468 Ma for late granitic intrusions in the Arequipa massif. Nd isotope considerations suggest that the Ilo magmatism involved variable contamination with an evolved continental crust ($\varepsilon Nd$ = -3.6 to -7.8; $T_{DM}$ = 1.5 to 1.8 Ga) with some evidence for mixing/mingling between magmas.

A Paleozoic metamorphic event is also recorded in the San Juán Marcona domain. Here (sample MAR-8), an event that produced variable Pb-loss of Grenvillian and Paleoproterozoic zircon is suggested by a discordia with a lower intercept at 469±70 Ma. Strong retrogression in the San Juán Marcona and Ocoña areas was attributed by Loewy et al. (2004) to an M3 tectonothermal event at *ca*. 465 Ma, i.e., Ordovician, as inferred from the U-Pb ages of alleged pre- and post-metamorphic plutons in the area. This event correlates with the

Marcona event of Shackleton et al. (1979), which produced a foliation (S3) and greenschist-facies retrogression of the basement gneisses. The Ocoña phyllonite zone that separates the Atico domain from the Camaná–Mollendo domain was attributed to this M3-S3 event (Shackleton et al., 1979; Loewy et al., 2004).

In the Ilo domain, zircons from the mylonitic dark gneiss and mylonitic porphyritic granite record evidence of overprinting at 430–440 Ma that could be related to retrogression within the shear zone. This age is within error of that found at San Juán Marcona and attests to metamorphic processes in Ordovician to Silurian times. This Ordovician to Silurian low-grade metamorphic overprint was largely restricted to shear zones and basement areas near the contact with cover sequences of Neoproterozoic age, such as in the San Juán Marcona domain (Shackleton et al., 1979; Chew et al., 2007). Focused flow of water-rich fluids along these zones played a significant role in metamorphism. Large areas of the Arequipa massif, however, do not record any evidence of Paleozoic metamorphism.

Correlations and geodynamic implications

There is agreement that the Laurentia and Amazonia cratons were juxtaposed across the Grenvillian orogenic belt at the end of Rodinia amalgamation at *ca*. 1.0 Ga (e.g., Dalziel, 1997; Davidson, 1995; Loewy et al., 2003; Tohver et al., 2004; Li et al., 2008). Models differ however on the relative position of these cratons, either in the NE (relative to present-day North America) or in the SE. Fig. 7 shows a paleomagnetically-constrained paleogeography at *ca*. 1.2 Ga, i.e., the alleged age of collision, according to Tohver et al. (2004). It shows the location of the Grenville belt of North America and its alleged counterpart along the western

and southwestern margin of Amazonia, together with outcrops of basement in the central Andes region with Grenvillian ages of interest to this contribution.

The Arequipa massif is a Paleoproterozoic inlier overprinted by the Grenvillian orogeny. Correlation with other Paleoproterozoic terranes in Laurentia or Amazonia is hindered by the isolation of the Arequipa massif. Compared with the ages of Paleoproterozoic orogenies in Laurentia (e.g., Goodge & Vervoort, 2006, fig. 1; Goodge et al., 2004, fig. 16) the age interval 1.76–2.1 Ga of Paleoproterozoic zircon in the San Juán and Camaná–Mollendo domains embraces the Yavapai orogeny (1.7–1.8 Ga) and the Penokean and Trans-Hudson orogenies (1.8–2.0 Ga; Schulz & Cannon, 2007; Whitmayer and Karlstrom, 2007). If formerly part of Laurentia, the Arequipa massif would be a relic of the pre-Grenvillian southern margin of the continent (present coordinates) isolated from the northern Paleoproterozoic belts by younger juvenile accretionary belts (Mazatzal and the Granite-Rhyolite province: 1.7–1.3 Ga; Fig. 7). The Laurentian connection was favoured by Wasteneys et al. (1995) and Loewy et al. (2003, 2004). On the other hand, rocks equivalent in age are also found in the Venturi–Tapajós belt of the Amazonia craton (2.0–1.8 Ga; Cordani and Teixeira, 2007). Nevertheless, the latter is a juvenile accretionary belt whilst the Arequipa massif is a block of reworked continental crust. Moreover the Venturi–Tapajós belt is quite distant from the Arequipa massif even in current reconstructions, which would imply a significant lateral displacement before Grenvillian metamorphism.

The Rio Apa block, south of present day Amazonia (Fig. 7), is another area to be considered, with U-Pb SHRIMP zircon ages largely coincident with those of detrital zircons in the Arequipa migmatitic gneisses (Cordani et al., 2008). Here widespread granitoid gneisses (1.94 Ga) were intruded by granitic plutons of the Alumiador Intrusive Suite (*ca*.

1.83 Ga) and younger orthogneisses between 1.7 and 1.76 Ga. Nd model ages are between 2.2 and 2.53 Ga (Cordani et al., 2005). Allegedly Paleoproterozoic metamorphism was medium- to high-grade (Cordani et al., 2008), but so far no evidence of UHT metamorphism has been recorded. The Rio Apa block was overprinted by a Grenville-age thermal event between *ca*. 1.3 and 1.0 Ga (Cordani et al., 2005) and with the Arequipa massif could thus be part of a larger Paleoproterozoic inlier within the South American counterpart of the Grenville orogen. The Maz domain in the Western Sierras Pampeanas of Argentina contains metasedimentary rocks with Paleoproterozoic zircons (1.7–1.9 Ga) and old Nd model ages (1.7–2.7 Ga), and was also reworked by the Grenvillian orogeny (Casquet et al., 2008), so that it could also be part of the same continental block.

Accretion of the Arequipa massif to Amazonia has been attributed to the Grenvillian (Sunsás) orogeny (Wasteneys et al., 1995; Loewy et al., 2004). Grenvillian ages of igneous rocks and metamorphism were early recognized along the southeastern margin of the Amazonia craton by Priem (1971) and Lintherland et al. (1989). The latter coined the name Sunsás orogeny for this tectonothermal event and attributed to it an age of *ca*. 1000 Ma. Orogeny involved folding and metamorphism along discrete metasedimentary belts that wrap around an older metamorphic core, the Rondonian–San Ignacio province (1.5–1.3 Ga; Cordani and Teixeira, 2007). Tohver et al. (2004) summarized the Grenvillian history as consisting of two events, an older one of Laurentia–Amazonia collision (1.2–1.12 Ga), and a younger one of alleged oblique convergence and intracontinental strike-slip at *ca*. 1.1 (Sunsás–Aguapei–Nova Brasilandia orogeny). The second event was accompanied by magmatism and metamorphism within the metasedimentary belts. Metamorphism was mostly of low grade but also reached granulitic facies (at Nova Brasilandia), dated at 1.09 Ga with cooling through 920 Ma. Precise U-Pb SHRIMP ages led Boger et al. (2005) to constrain

Sunsás deformation as predating *ca*. 1070 Ma. Santos et al. (2008) revisited the tectonic evolution of the southern margin of Amazonia and re-interpreted the Sunsás orogeny as an autochthonous orogen involving four orogenic pulses between 1465 and 1110 Ma, suggesting a Laurentia–Amazonia connection at *ca*. 1450 Ma. The period between 1070 Ma and *ca*. 980 Ma was apparently a period of craton stabilization, with anorogenic granitic magmatism along the southern margin of Amazonia (Santos et al., 2008; Cordani and Teixeira, 2007, and references therein).

In the Grenville province of Canada the Grenvillian orogenic cycle started at *ca*. 1.25 Ga and ended at *ca*. 850 Ma (Davidson, 1995, Rivers, 1997). Between 1100 and *ca*. 980 Ma, the orogenic cycle involved two contractional episodes: the widespread penetrative Ottawan orogeny (1080–1020 Ma) and the more localized Rigolet event (1000–980 Ma). In a recent interpretation of the crustal-scale orogenic evolution of the Grenville province, Rivers (2008) argued that collapse of the Ottawan thickened orogen took place during the time interval 1050–1020. Former contractional structures were reworked in extension and AMGC complexes were intruded that heated the middle crust. Horst-and-graben structures developed at this time in the upper crust. During the time interval 1020–950 Ma the Grenville province underwent contraction at the Grenville front. The hinterland however underwent protracted extensional collapse over this period with development of extensional shear zones, deep ductile detachments and metamorphism (Rivers, 2008).

The contractional phase of the Ottawan orogeny (1080–1050 Ma) and the older Grenvillian orogenic cycle events are not recognized in the Arequipa massif. However, the coincidence of the Arequipa massif Grenvillian metamorphic ages of 1040–840 Ma with protracted extension both in the Laurentian Grenville orogen (except for the localized Rigolet pulse at *ca*. 1.0 Ga)

and in southern Amazonia suggests that metamorphism in Arequipa, which was low-P type, might be related to overall extension and heating, and not to collision as formerly argued. The precise tectonic setting remains unknown and more structural work is required to constrain it. Laurentia–Amazonia collision took probably place earlier, at *ca*. 1.2 Ga (Tohver et al., 2004) or during the Ottawan orogeny (Rivers, 1977, 2008) but is not recognized in the Arequipa massif except for the detrital zircons of 1200–1260 Ma in the Atico metasedimentary rocks. Whether formerly part of Laurentia or of Amazonia, the location of Arequipa before collision remains uncertain.

The Atico sedimentary basin that formed between 1200 and 1000 Ma might be also related to the protracted extensional event referred to above. The magmatism at Ilo that included anorthosites was not involved in the Grenvillian metamorphism. Grenvillian metamorphic domains with different P-T-t histories were probably juxtaposed across low-grade shear zones in the Ordovician–Silurian.

## Conclusions

The Arequipa massif is a Paleoproterozoic inlier in the South American Grenville-age orogen. It was probably part of a larger continental block that also included the Río Apa block and the western Sierras Pampeanas Maz terrane.

The Paleoproterozoic pattern that emerges is one of an orogeny between *ca*. 1.79 and 2.1 Ga (Orosirian to Rhyacian) involving: a) early magmatism (between 1.89 and 2.1Ga), presumably through partly Archaean continental crust, b) sedimentation of a thick sequence

of terrigenous sediments, c) UHT metamorphism at *ca*. 1.87 Ga, and d) late felsic magmatism at *ca*. 1.79 Ga.

The Atico domain can be interpreted as a sedimentary basin deposited on a Paleoproterozoic high-grade basement consisting of igneous and metamorphic rocks. Deposition occurred between *ca*. 1200 and *ca*.1000 Ma, i.e., in the Late Mesoproterozoic. Detrital zircons were fed from a source area similar to the high-grade Camaná–Mollendo and San Juán domains, but also from an unknown source that provided Mesoproterozoic zircons of 1260 –1600 Ma.

Grenville-age metamorphism at Arequipa took place in up to three stages: 1) *ca*. 1040 Ma in the Quilca and Camaná areas of the Camaná–Mollendo domain, and in the San Juán Marcona domain, 2) 940±6 Ma in the Mollendo area of the Camaná–Mollendo domain; 3) between 1000 and 850 Ma in the Atico domain. In the Arequipa massif metamorphic domains are therefore juxtaposed that underwent different Grenvillian metamorphic histories. The geodynamic significance of Grenvillian metamorphism is unknown but it could be related to extension and not to collision as formerly argued.

During the early Paleozoic the Arequipa massif underwent magmatism at *ca*. 465 Ma and focused retrogression along shear zones or unconformities between 430 and 440 Ma.

**Acknowledgements**

Financial support for this work was provided by Spanish MEC grant CGL2005-02065/BTE and Universidad Complutense grant 910495 and Argentinian PICT 1009. We are

grateful to Instituto Geológico Minero y Metalúrgico (INGEMMET) of Perú, and particularly to Dr. Victor Carlotto, who helped us with the fieldwork.

## References

Arima, M, and Gower, Ch.F., 1991. Osumilite-bearing granulites in the eastern Grenville Province, Eastern Labrador, Canada: Mineral parageneses and metamorphic conditions. Journal of Petrology, 32, 1, 29-61.

Black L.P., Williams, I.S., Compston, W., 1986. Four zircon ages from one rock: the history of a 3930 Ma old granulite form the Mt. Stones, Enderby Land, Antarct*ica*. Contributions to Mineralogy and Petrology, 94, 427-437.

Bock, B., Bahlburg, H., Wörner, G., Zimmerman, U., 2000. Tracing crustal evolution in the Southern Central Andes from Late Precambrian to Permian with geochemical and Nd and Pb data. Journal of Geology, 108, 515-535.

Boger, S.D., Raetz, M., Giles, D., Etchart, E., Fanning, C.M., 2005. U-Pb data from the Sunsas region of Eastern Bolivia, evidence for an allocthonous origin of the Paragua block. Precambrian Research, 139, 121-146.

Carson, C.J., Ague, J.J., Coath, C.D., 2002. U-Pb geochronology from Tonagh Island, East Antarctica: Implications fro the timing of ultra-high temperature metamorphism of the Napier Complex. Precambrian Research, 116, 237-263.

Casquet, C., Pankhurst, R.J., Rapela, C., Galindo, C., Fanning, C.M., Chiaradia, M., Baldo, E., González-Casado, J.M., Dahlquist, J.A., 2008. The Maz terrane: a Mesoproterozoic domain in the western Sierras Pampeanas (Argentina) equivalent to the Arequipa-Antofalla

block of southern Peru? Implications for Western Gondwana margin evolution. Gondwana Res., 13, 163-175.

Chew, D.M., Schaltegger, U., Kosler, J., Whitehouse, M.J., Gutjahr, M., Spikings, R.A., Miskovic, A., 2007. U-Pb geochronologic evidence for the evolution of the Gondwanan margin of the north-central Andes. Geological Society of America Bulletin, 119, 697-711.

Cobbing, E.J., Pitcher, 1972. Plate tectonics and the Peruvian Andes. Nature, 246, 51-53.

Cobbing, E.J., Ozard, J.M., Snelling, N.J., 1977. Reconnaisance geochronology of the crystalline basement of the Coastal Cordillera of southern Peru. Geological Society of America Bulletin, 88, 241-246.

Copeland, P., Parrish, R.R., Harrison, T.M.,1988. Identification of inherited radiogenic Pb in monazite and its implications for U-Pb systematics. Nature, 333, 760-763.

Cordani, U.G., Teixeira, W., 2007. Proterozoic accretionary belts in the Amazonian Craton. In: Hatcher, R.D. Jr., Carlson, M.P. McBride, J.H., Martinez Catalán, J.R. (Eds.), 4-D Framework of Continental Crust: Geological Society of America, Memoir 200, 297-320.

Cordani, U.G., Tassinari, C.C.G., Reis Rolim, D.R., 2005. The basement of the Rio Apa Craton in Mato Grosso do Sul (Brazil) and northern Paraguay: a geochronological correlation with tectonic provinces of the south-western Amazonian Craton. In: Pankhurst, R.J. & Veiga, G.D. (Eds.), Gondwana 12: Geological and Biological Heritage of Gondwana. Abstracts, Academia Nacional de Ciencias, Córdoba, Argentina, p.113.

Cordani, U.G., Tassinari, C.C.G., Teixeira, W., Coutinho, J.M.V., 2008. U-Pb SHRIMP Zircon ages for the Rio Apa cratonic fragment in Mato Grosso do sul (Brazil) and northern Paraguay: Tectonic implications. VI South American Symposium on Isotope Geology, Bariloche, Argentina, Proceedings.

Corfu, F., Hanchar, J.M., Hoskin, W.O., Kinny, P., 2003. Atlas of Zircon Textures. In: Hanchar, J.M. and Hoskin, P.W.O. (Eds.), Zircon, Reviews in Mineralogy and Geochemistry, 53, 469-500.

Dahlquist, J.A., Pankhurst, R.J., Rapela, C.W., Galindo, C., Alasino, P., Fanning, C.M., Saavedra, J., Baldo, E., 2008. New SHRIMP U-Pb data from the Famatina Complex: constraining Early-Mid Ordovician Famatinian magmatism in the Sierras Pampeanas, Argentina. Geologica Acta, 6, 319-333.

Dalmayrac, B., Lancelot, J.R., Leyreloup, A., 1977. Two-billion year granulites in the Late Precambrian metamorphic basement along the southern Peruvian coast. Science, 198, 49-51.

Dalziel, I. W. D., 1997. Overview. Neoproterozoic-Paleozoic geography and tectonics: Review, hypothesis, environmental speculation: Geological Society of America Bulletin, 109, p. 16-42.

Davidson, A., 1995. A review of the Grenville orogen in its North American type area. *Journal of Australian Geology and Geophysics*, 16, 3-24.

DePaolo, D.J., 1981. Neodymium isotopes in the Colorado Front Range and crust-mantle evolution in the Proterozoic. Nature, 291, 193-196.

DePaolo, D.J., Linn, A.M., Schubert, G., 1991. The continental crustal age distribution: methods of determining mantle separation ages from Sm-Nd isotopic data and application to the Southwestern United States. J. Geophys. Res., B96, 2071-2088.

Goodge, J.W., Vervoort, J.D., 2006. Origin of Mesoproterozoic A-type granites in Laurentia: Hf isotope evidence. Earth and Planatery Science Letters, 243, 711-731.

Goodge, J.W., Fanning, M., Bennett, V.C., 2001. U-Pb evidence of ~ 1.7 Ga crustal tectonism during the Nimrod Orogeny in the Transantarctic Mountains, Antarctica: implications for Proterozoic plate reconstructions. Precambrian Research, 112, 261-288.

Goodge, J.W., Williams, I.S., Myrow, P., 2004. Provenance of Neoproterozoic and lower Paleozoic siliciclastic rocks of the Central Ross orogen, Antarctica: detrital record of rift-, passive-, and active-margin sedimentation. Geological Society of America Bulletin, 116, 1253-1279.

Hoffman, P.F., 1991. Did the breakout of Laurentia turn Gondwanaland inisde out? Science, 252, 1409-1412.

Li, Z.X., et al., 2008, Assembly, configuration, and break-up history of Rodinia: A synthesis. Precambrian Research, 160, 179-210.

Litherland, M., Annells, R.N., Darbyshire, D.P.F., Fletcher, C.J.N., Hawkins, M.P., Klinck, B.A., Mitchell, W.I., O´Connor, E.A., Pitfield, P.E.J., Power, G., Webb, B.C., 1989. The Proterozoic of eastern Bolivia and its relationships to the Andean mobile belt. Precambrian Research, 43, 157-174.

Loewy, S.L., Connelly, J.N., Dalziel, I.W.D. & Gower, C.F., 2003. Eastern Laurentia in Rodinia: constraints from whole-rock Pb and U/Pb geochronology. *Tectonophysics*, 375, 169-197.

Loewy, S.L., Connelly, J.N. & Dalziel, I.W.D., 2004: An orphaned block: the Arequipa-Antofalla basement of the central Andean margin of South America. *GSA Bulletin*, 116, 171-187.

Ludwig, K.R., 2001. SQUID 1.02. A user´s manual. Berkeley Geochronological Center Special Publication, 2, 2455 Ridge Road, Berkeley, Ca 94709, USA.

Martignole, J., Martelat, J.E., 2003. Regional-scale Grenvillian-age UHT metamorphism in the Mollendo-Camana Block (basement of the Peruvian Andes). Journal of Metamorphic Geology, 21 (1), 99-120.

Martignole, J., Stevenson, R., Martelat, J.E., 2005. A Grenvillian anorthosite-mangerite-charnockite-granite suite in the basement of the Andes: the Ilo AMCG site (souhern Peru). IDSAG, Barcelona, Extended Abstracts, 481-484.

Moores, E.M., 1991. Southwest U.S.-East Antarctic (SWEAT) connection: A Hypothesis. Geology, 19, 425-428.

Pankhurst, R.J., Rapela, C.W., Fanning, C.M., 2000. Age and origin of coeval TTTG, I- and S-type granites in the Famatinian belt of NW Argentina. Transactions of the Royal Society of Edimburgh: Earth Sciences 91, 151-168.

Parrish, R.R.,1990. U-Pb dating of monazite and its application to geological problems. Canadian Journal Earth Sciences, 270, 1431-1450.

Priem, H.N.A., Boelrijk, N.A.I.M., Hebeda, E.H., Verdumen, E.A.T., Verschure, R.H. and Bon, E.H., 1971. Granitic complexes and associated tin mineralization of Grenville age in Rondonia, western Brasil. Geological Society of America Bulletin, 82, 4, 1095-1102.

Ramos, V.A., 1988. Late Proterozoic – Early Paleozoic of South America – a collisional history. Episodes, 11, 168-174.

Restrepo-Pace P.A., Ruiz, J., Gehlers, G., Cosca, M., 1997. Geochronology and Nd isotopic data of Grenville-age rocks in the Colombian Andes: new constraints fro Late Proterozoic – Early Paleozoic paleocontinental reconstructions of the Amercias. Earth and Planetary Science Letters, 150, 427-441.

Rivers, T., 1997, Lithotectonic elements of the Grenville Province: review and tectonic implications. Precambrian Research, 86, 117-154.

Rivers, 2008. Assembly and preservation of lower, mid and upper orogenic crust in the Grenville Province – Implications for the evolution of large hot long-duration orogens. Precambrian Research, 167, 237-259.

Santos, J.O.S., Rizzotto, G.J., Potter, P.E., McNaughton, N.J., Matos, R.S., Hartmann, L.A., Chemale, F. Jr., Quadros, M.E.S., 2008. Age and autochtonous evolution of the Sunsás Orogen in West Amazon Craton based on mapping and U-Pb geocronology. Precambrian Research, 165, 120-152.

Shackleton, R.M., Ries, A.C., Coward, M.P., Cobbold, P.R. 1979. Structure, metamorphism and geochronology of the Arequipa massif of coastal Peru. Journal of the Geological Society, London, 136, 195-214.

Schulz , K.L., Cannon, W.F., 2007. The Penokean orogeny in the Lake Superior region. Precambrian Research, 157, 4-25.

Siivola, J., Schmid, R., 2007. List of Mineral Abbreviation. In: Fettes, D., Desmonds, J. (Eds.). Metamorphic Rocks. A Classification and Glossary of Terms. Cambridge University Press, p. 93-110.

Taylor, S.R., McLennan, S.M., 1988. The significance of the Rare Earths in geochemistry and cosmochemistry. In: Gschneider, K.A. Jr. and Eyring, L. (Eds.), Handbook on the Physics and Chemistry of Rare Earths, Elsevier Publ. B.V., 11, 486-578.

Tohver, E., Bettencourt, J.S., Tosdal, R., Mezger, K., Leite, W.B. and Payolla, B.L., 2004. Terrane transfer during Grenville orogeny: tracing the Amazonian ancestry of southern Appalachian basement through Pb and Nd isotopes. Earth and Planetary Science Letters, 228, 161-176.

Tosdal, R.M., 1996. The Amazon-Laurentian connection as viewed from the Middle Proterozoic rocks in the Central Andes, western Peru and Northern Chile. Tectonics, 15, 827-842.

Vavra, G., Schmid, R., Gebauer, D., 1999. Internal morphology, habit and U-Th-Pb microanalysis of amphibolite-to-granulite facies zircons: geochronology and the Ivrea Zone (Southern alps). Contributions to Mineralogy and Petrology, 134, 380-404.

Wasteneys, H.A., Clark, A.H., Farrar, E., Langridge, R.J., 1995. Grenvillian granulite-facies metamorphism in the Arequipa Massif, Peru: a Laurentia-Gondwana link. Earth and Planetary Science Letters, 132, 63-73.

Whitmayer, S.J., Karlstrom, K.E., 2007. Tectonic model for the Proterozoic growth of North America. Geosphere, 3, 220-259.

Williams, I.S., 1998. U-Th-Pb geochronology by ion microprobe. In: McKibben, M.A., Shanks, W.C. III, Ridley, W.I. (Eds.), Applications of microanalytical techniques to understanding mineralizing processes. Rev. Econ. Geol., 7, 1-35.

**Figures**

Fig. 1 Sketch map of the Arequipa Massif showing domains distinguished in the text and location of samples. Insets show the location of the Arequipa Massif in South America and relationships with other pre-Andean outcrops in northern Chile and Argentina.

Fig. 2. a) Banded migmatitic gneisses near Quilca traversed by Cainozoic basaltic dykes. b) Basement outcrop near Ilo. Mylonitic porphyritc granites (P) with disrupted anorthosite lenses (A), and dark bands of fine-grained mylonitic gneisses (M).

Fig. 3. U–Pb SHRIMP data for samples from the northern section of the Arequipa Massif. $^{204}$Pb-corrected data are plotted as 1σ error ellipses in Wetherill Concordia diagrams, with typical cathodo-luminescence images displayed below. (a) MAR-8 (San Juán Marcona) shows data for cores (grey shading) trending away from *ca*. 1800 Ma, interpreted as an

igneous protolith age, and rims (white ellipses) plotting on a Discordia between *ca*. 1000 Ma (Grenvillian age of main metamorphism) towards *ca*. 470 Ma (Famatinian overprint). (b) OCO-26 (Atico) shows a rather discordant spread of data from Archaean to Neoproterozoic, with the $^{207}Pb/^{206}Pb$ ages concentrating at *ca*. 1000 Ma (metamorphism).

Fig. 4. U–Pb SHRIMP data for samples from the southern section of the Arequipa Massif. $^{204}Pb$-corrected data are plotted as 1σ error ellipses in Wetherill Concordia diagrams, with typical cathodo-luminescence images displayed below. (a) CAM-2 shows a strong bipolar distribution of ages ($^{206}Pb/^{238}U$ for <1000 Ma, $^{207}Pb/^{206}Pb$ for >1000 Ma), indicating Pb-loss from a major events at *ca*. 1900 Ma and a second concentration around 1000 Ma. (b) CAM-7 and (c) QUI-16 show similar patterns with additional discordance (white ellipses indicate data ignored in the discordia fit). (d) MOL-17 from the Mollendo area (cathodo-luminescence image shown below) also has three highly concordant data points for zircon rims at 940 Ma.

Fig. 5. U–Pb SHRIMP data for samples from the Ilo domain. Uncorrected data are plotted as 1σ error ellipses in Tera-Wasserburg diagrams. All data plot with Ordovician extrapolated ages, but with a significant spread along Concordia. For (a) ILO-19 and (b) ILO-20, the insets show attempts at unmixing the ages. For (c) ILO-23 (anorthosite) insufficient data were obtainable for detailed treatment, but the cathodo-luminescence image inset shows good igneous concentric zoning to support interpretation of the magmatic crystallization as Ordovician in age.

Fig. 6. Chondrite-normalized REE patterns of migmatitic gneisses. The North America Shale Composite REE pattern (Taylor and McLennan, 1988) is added for comparison.

Fig. 7. Paleogeographical reconstruction of Laurentia and Amazonia at *ca*. 1.2 Ga (Tohver et al., 2004), showing Precambrian orogenic belts with ages according to Goodge et al. (2004, fig. 16), Tohver et al. (2004) and Cordani and Teixeira (2007). Outcrops of basement with Grenvillian ages in southern Laurentia and in the Central Andean region (Peru, NW Chile and Argentina) have been included (the latter in its present position relative to Amazonia). Laurentia: TH, Trans Hudson and related mobile belts; P, Penokean orogen; Y, Yavapay orogen; M, Mazatzal orogen; GR, Granite-Rhyolite province; FM, Franklin mountains outcrop; VHM, Van Horn Mountains outcrop; LU, Llano Uplift outcrop. Amazonía: MI, Maroni–Itacaiunas Province; CA, Central Amazonia province; VT, Venturi-Tapajós province; RNJ, Rio Negro Jurena province; R, Rondonia–San Ignacio province; Sunsás, orogenic belts of Grenvillian age along southern Amazonía; AM, Arequipa Massif (Peru); RA, Rio Apa outcrop (Brasil, Paraguay); WSP, Western Sierras Pampeanas (Argentina); G, Garzón massif (Colombia); ST, Santander massif (Colombia).

Figure1

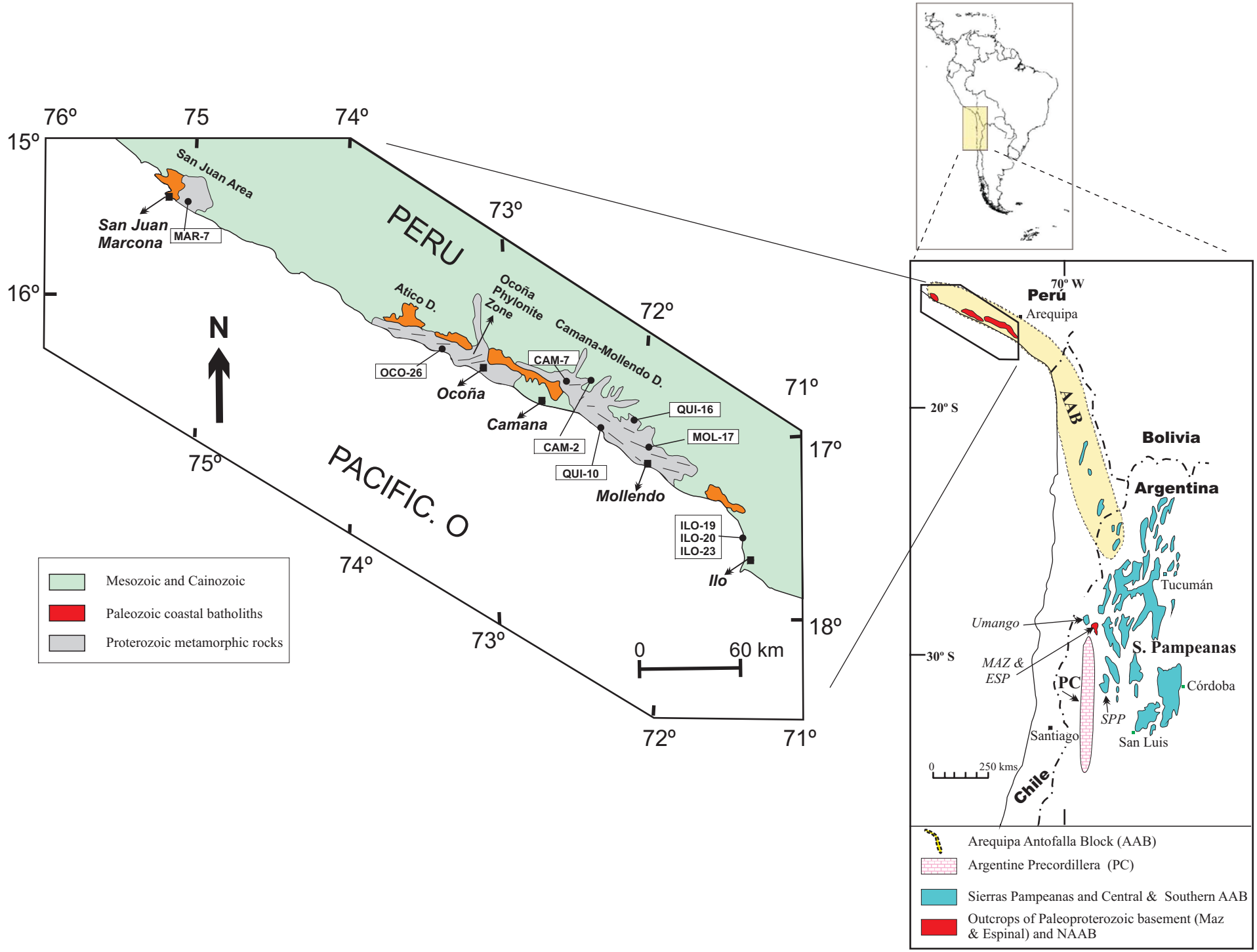


Fig. 1


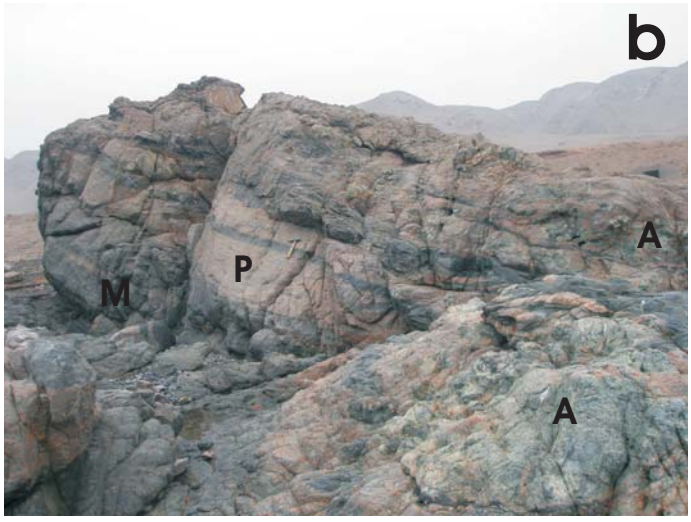


Fig. 2

**Figure3**

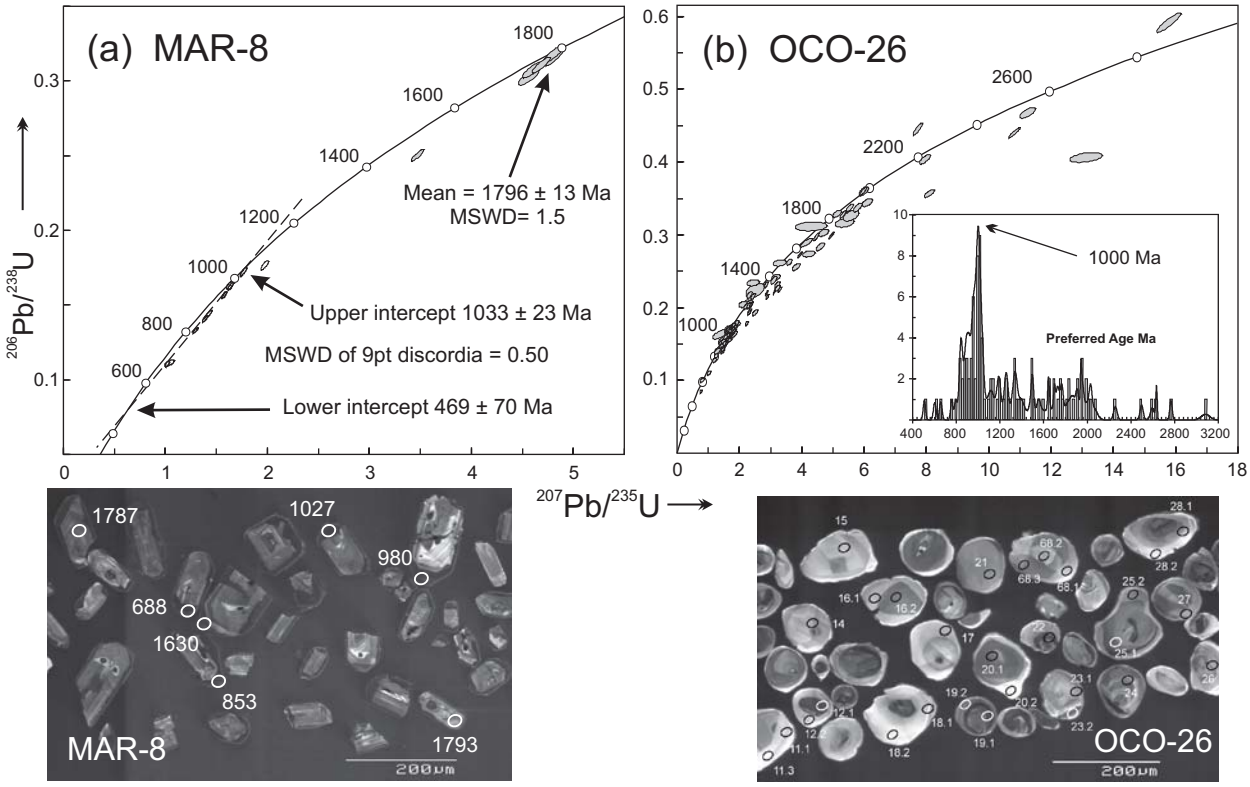


Casquet et al. Fig 3

**Figure4**

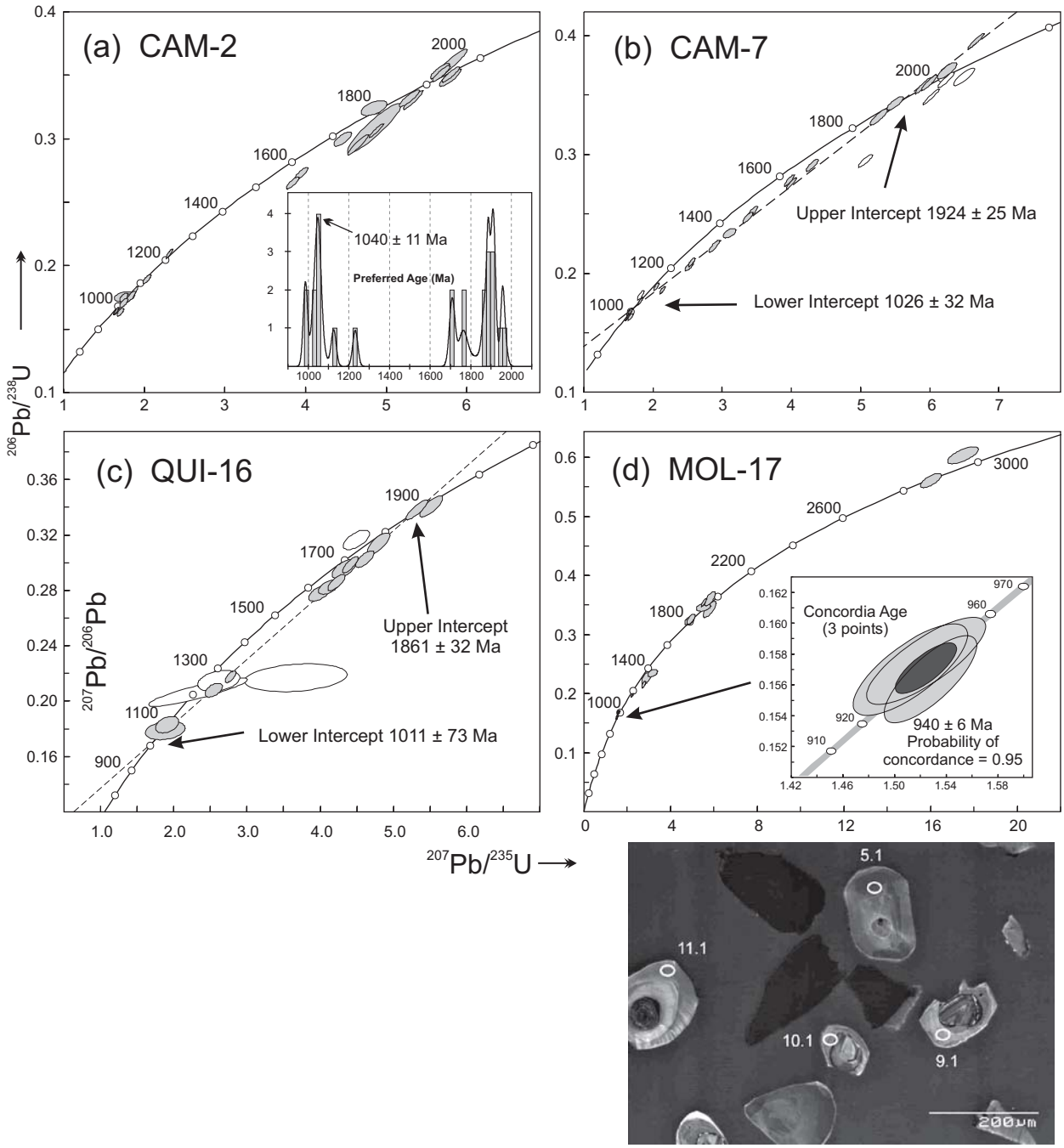


Casquet et al. Fig 4

**Figure5**

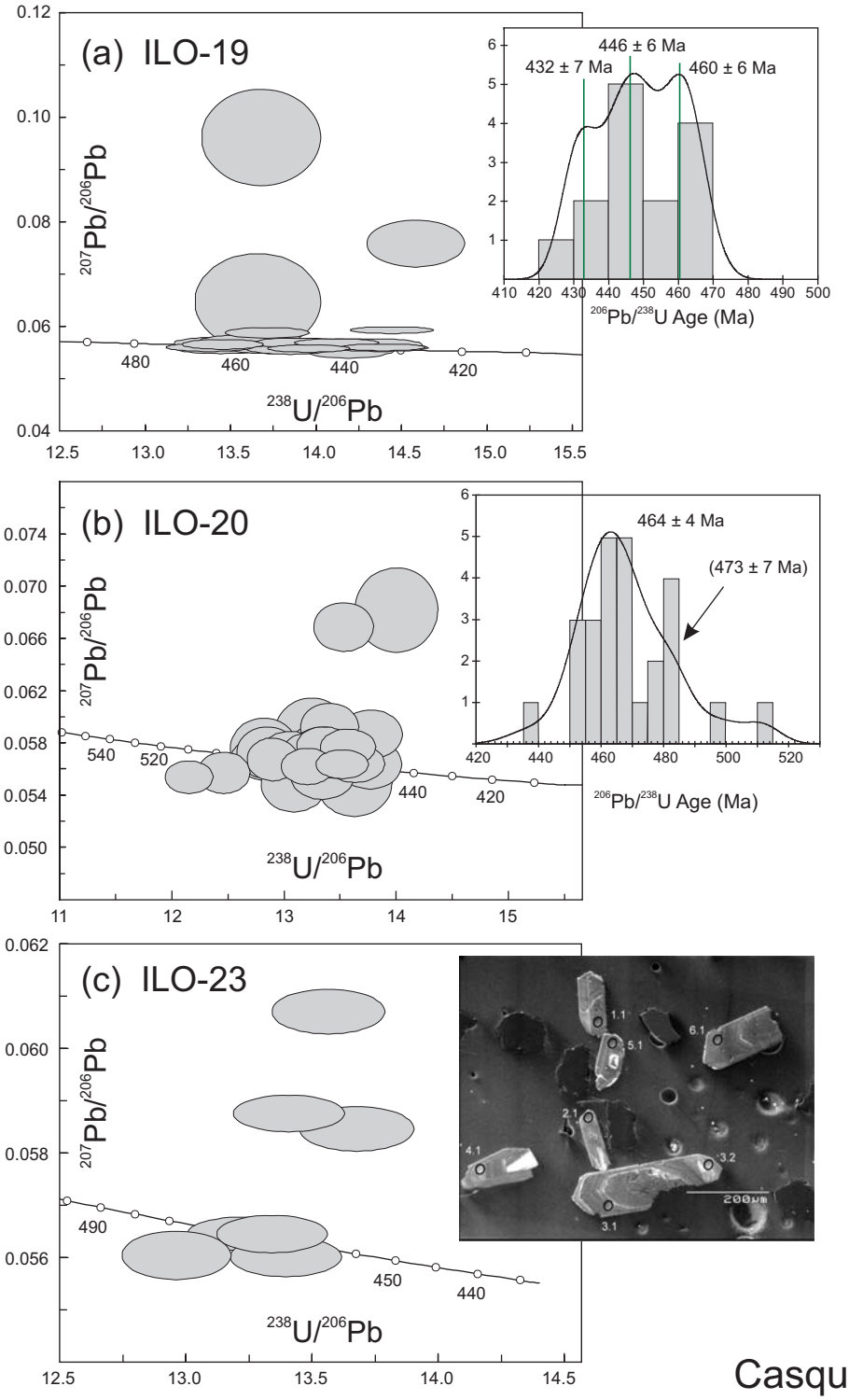


Casquet et al. Fig 5
(one column)

Figure6

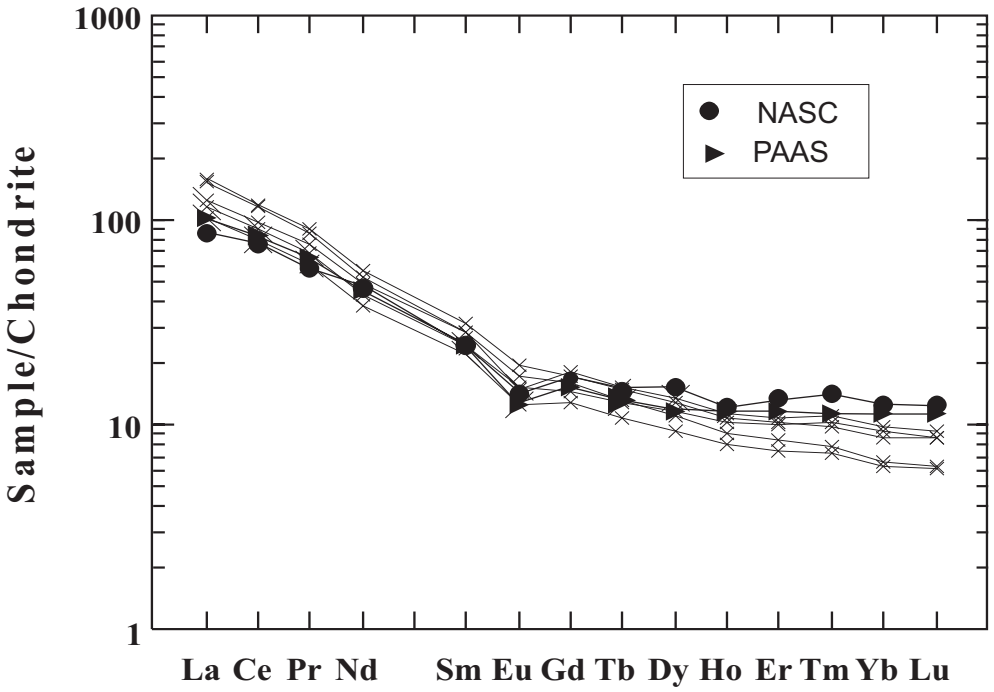


Fig.6

Figure7

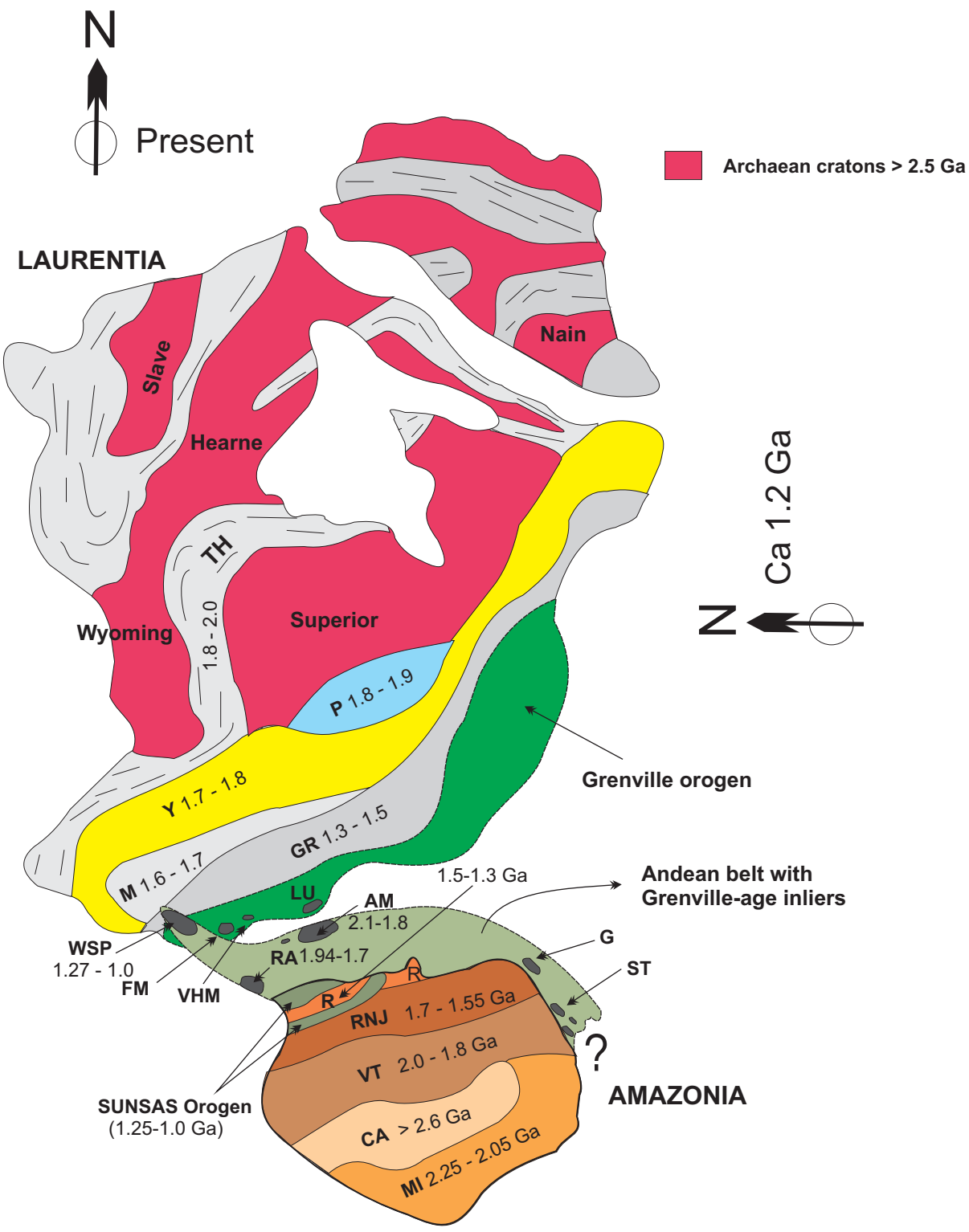


Fig. 7

**Table1**

**TABLE 1.Short description of rocks selected for U-Pb SHRIMP zircon dating and geochemistry**

| Sample | coordinates | domain | rock type* | abreviated mineralogy** | Anal. work |
|---|---|---|---|---|---|
| MAR-8 | 15º24´21.3´´S, 75º08´16.8´´W | S. Juan Marcona | Fine-grained gneiss. Dacitic to rhyodacitic. Low-grade retrogression: strong | Qtz, Pl, Kfs, Ms, Chl, Op, Cb, Zrn | S |
| OCO-26 | 16º26´32.5´´S, 73º07´24.7´´W | S. Juan Marcona | Medium-grade metasandstone | Qtz, Pl, Ms, Bt, Zrn | S |
| CAM-2 | 16º32´17.2´´S, 72º31´23.2´´W | Camaná-Mollendo | Banded migmatitic gneiss | Qtz, Pl, Kfs, Opx, Sil, Bt, Mag, Zrn | S, I, R |
| CAM-6 | 16º30´40.3´´S, 72º38´16.6´´W | "" | Gneiss (mesosome) | Qtz, Kfs, Pl, Grt, Sill, Mag, Bt, Chl, Ser, Zr, Ap, Sp | I, R |
| CAM-7 | 16º30´40.3´´S, 72º38´16.6´´W | Camaná-Mollendo | Banded migmatitic gneiss | Qtz, Kfs, Pl, Grt, Sil, Bt, Mag, Zrn | S, I, R |
| QUI-10 | 16º42´52.9´´S, 72º25´18.9´´W | "" | Banded migmatitic gneiss | Qtz, Kfs, Sill, Bt, Opx, Pl, Mag, Chl, Ser, Zrn, Ap | I, R |
| QUI-16 | 16º40´59.3´´S, 72º20´05.9´´W | "" | Banded migmatitic gneiss | Qtz, Pl, Kfs, Bt, Sill, Grt, Mag, Ser, Chl, Zrn | S,I, R |
| MOL-17 | 16º54´59.2´´S, 72º02´50.4´´W | Camaná-Mollendo | Augen-gneiss | Qtz, Kfs, Pl, Grt, Sil, Mag, Bt, Ser, Ep, Chl, Zrn | S |
| ILO-19 | 17º27´59.2´´S, 71º22´19.9´´W | Ilo | Reddish mylonitic porphyritic granite. Low-grade retrogression: strong | Qtz, Chl, Ep, Pl, Kfs, Ttn, Ilm, Ser, Aln, Ap, Fl, Zr | S, I, R |
| ILO-20 | 17º27´59.2´´S, 71º22´19.9´´W | Ilo | Mylonitic dark gneiss. Low grade retrogression: moderate | Qtz, Pl, Hb, Bt, Chl, Ser, Ep, Aln, Mt, Ap, Zrn | S, I, R |
| ILO-23 | 17º28´56.1´´S, 71º21´56.4´´W | Ilo | Coarse grained anorthosite. Low grade retrogression: minor | Pl, Hb, Bt, Ttn, Rt, Ilm, Ser, Chl, Ep | S, I, R |

* For a detailed description see supplementary table in Data Repository

**Mineral abreviations according to Siivola and Schmid (2007). Order reflects relative modal amounts.

Analytical work: S = U-Pb SHRIMP; I = Nd isotope composition; R = REEs chemical analysis

Table2

**Table 2. Sm-Nd isotope composition of selected rocks from the Camana-Mollendo and Ilo domains.**

| Sample | Sm ppm | Nd ppm | Sm/Nd | $^{147}Sm/^{144}Nd$ | $^{143}Nd/^{144}Nd$ | $eNd_{465}$ | $T_{DM\ (465)}^{*}$ | $eNd_{1000}$ | $eNd_{1700}$ | $T_{DM}$ |
|---|---|---|---|---|---|---|---|---|---|---|
| CAM-2 | 5.59 | 30.3 | 0.1845 | 0.1115 | 0.511333 | | | -14.6 | -6.9 | 2445 |
| CAM-6 | 6.57 | 34.4 | 0.1910 | 0.1154 | 0.511348 | | | -14.8 | -7.5 | 2513 |
| CAM-7 | 5.1 | 27.1 | 0.1882 | 0.1137 | 0.511294 | | | -15.6 | -8.2 | 2549 |
| QUI-10 | 7.3 | 39.9 | 0.1830 | 0.1106 | 0.511322 | | | -14.7 | -6.9 | 2440 |
| QUI-16 | 6.57 | 37.5 | 0.1752 | 0.1059 | 0.511343 | | | -13.7 | -5.5 | 2314 |
| ILO-19 | 8.01 | 50.7 | 0.1580 | 0.0955 | 0.511996 | -6.4 | 1691 | | | |
| ILO-20 | 10 | 60 | 0.1667 | 0.1007 | 0.511940 | -7.8 | 1791 | | | |
| ILO-23 | 1.02 | 4.46 | 0.2287 | 0.1383 | 0.512274 | -3.6 | 1483 | | | |

Nd isotopic ratios were normalized to $^{146}Nd/^{144}Nd = 0.7219$.

La Jolla Nd standard gave a mean $^{143}Nd/^{144}Nd$ of 0.511847 ± 0.00001 (n = 9).

The 2σ analytical errors are 0.1% in $^{147}Sm/^{144}Nd$ and 0.006% in $^{143}Nd/^{144}Nd$.

Decay constant was λSm = 6.54x10-12 a-1.

$T_{DM}$* is model age according to DePaolo *et al.* (1991).

$^{147}Sm/^{144}Nd$ and $^{143}Nd/^{144}Nd$ values assumed to be 0.1967 and 0.512636 for CHUR, and 0.222 and 0.513114 for depleted mantle respectively

**Table 3. Rb-Sr composition of muscovite from pegmatites**

| Sample | Rb | Sr | Rb/Sr | $^{87}Rb/^{86}Sr$ | $^{87}Sr/^{86}Sr$ | model age Ma |
|---|---|---|---|---|---|---|
| JC-01C Ms | 609.412 | 6.52 | 93.4681 | 463.637 | 8.011008 | 1100 |
| QUI-005 Ms | 526.469 | 6.664 | 79.0020 | 338.286 | 5.614221 | 1015 |

Sr isotopic ratios were normalized to $^{86}Sr/^{88}Sr = 0.1194$.

NBS987 standard gave a mean $^{87}Sr/^{86}Sr$ ratio of $0.710216 \pm 0.00005$ (n = 10).

The $2\sigma$ analytical errors are 1% in $^{87}Rb/^{86}Sr$,0.01% in $^{87}Sr/^{86}Sr$.

Decay constants used were $\lambda Rb = 1.42x10\text{-}11$ a-1.

Model ages assumes initial $^{87}Sr/^{86}Sr$ values between 0.703 and 0.715

**Table 4. REE analyses of granulites**

| | CAM-2 | CAM-6 | CAM-7 | QUI-10 | QUI-16 |
|---|---|---|---|---|---|
| La | 42.8 | 46.4 | 37.7 | 58.1 | 55.3 |
| Ce | 86.1 | 93.2 | 76.8 | 115 | 110 |
| Pr | 9.46 | 10.5 | 8.43 | 12.4 | 11.8 |
| Nd | 30.3 | 34.4 | 27.1 | 39.9 | 37.5 |
| Sm | 5.59 | 6.57 | 5.1 | 7.3 | 6.57 |
| Eu | 1.32 | 1.28 | 1.1 | 1.71 | 1.5 |
| Gd | 4.44 | 5.54 | 3.94 | 5.32 | 4.88 |
| Tb | 0.75 | 0.89 | 0.63 | 0.86 | 0.76 |
| Dy | 4.44 | 5.09 | 3.56 | 4.93 | 4.21 |
| Ho | 0.88 | 0.96 | 0.68 | 0.92 | 0.77 |
| Er | 2.49 | 2.72 | 1.84 | 2.55 | 2.1 |
| Tm | 0.364 | 0.393 | 0.257 | 0.345 | 0.277 |
| Yb | 2.28 | 2.42 | 1.57 | 2.15 | 1.62 |
| Lu | 0.333 | 0.351 | 0.235 | 0.326 | 0.241 |
| REE | 191.5 | 210.7 | 168.9 | 251.8 | 237.5 |
| | | | | | |
| (La/Yb)N | 13.5 | 13.8 | 17.2 | 19.4 | 24.5 |
| (La/Sm)N | 4.9 | 4.6 | 4.8 | 5.1 | 5.4 |
| (Gd/Yb)N | 1.6 | 1.9 | 2.1 | 2.0 | 2.5 |
| Eu/Eu* | 0.8 | 0.6 | 0.8 | 0.8 | 0.8 |

**e-component1**

**Click here to download e-component: Supplementary data #1.pdf**

**e-component2**

**Click here to download e-component: Supplementary data # 2.pdf**